BBA - Molecular Basis of Disease 1870 (2024) 167350

Contents lists available at ScienceDirect

BBA - Molecular Basis of Disease

journal homepage: www.elsevier.com/locate/bbadis

Exposure to serum from exclusive heated tobacco product smokers induces mTOR activation and fibrotic features in human cardiac stromal cells

Vittorio Picchio [a,b,1], Francesca Pagano [c,1], Roberto Carnevale [a,b], Alessandra D'Amico [d], Claudia Cozzolino [a], Erica Floris [a], Antonella Bordin [a], Leonardo Schirone [b], Daniele Vecchio [a], Wael Saade [e], Fabio Miraldi [e], Elena De Falco [a,f], Sebastiano Sciarretta [a,b], Mariangela Peruzzi [e,f], Giuseppe Biondi-Zoccai [a,f], Giacomo Frati [a,b], Isotta Chimenti [a,f,*]

[a] Department of Medical Surgical Sciences and Biotechnologies, Sapienza University, Latina, Italy
[b] Department of AngioCardioNeurology, IRCCS Neuromed, Pozzilli, Italy
[c] Institute of Biochemistry and Cell Biology, National Council of Research (IBBC-CNR), Monterotondo, Italy
[d] Department of Movement, Human, and Health Sciences, University of Rome "Foro Italico", Rome, Italy
[e] Department of Clinical, Internal Medicine, Anesthesiology and Cardiovascular Sciences, Sapienza University, Rome, Italy
[f] Maria Cecilia Hospital, GVM Care & Research, Cotignola, Italy

ARTICLE INFO

Keywords:
Heat-not burn cigarettes
Cardiac fibrosis
Smoking
Cardiac fibroblast
mTOR pathway
Atrial fibrillation

ABSTRACT

Chronic smokers have increased risk of fibrosis-related atrial fibrillation. The use of heated-tobacco products (HTPs) is increasing exponentially, and their health impact is still uncertain. We aim to investigate the effects of circulating molecules in exclusive HTP chronic smokers on the fibrotic behavior of human atrial cardiac stromal cells (CSCs). CSCs were isolated from atrial tissue of elective cardiac surgery patients, and exposed to serum lots from young healthy subjects, stratified in exclusive HTP smokers, tobacco combustion cigarette (TCC) smokers, or nonsmokers (NS). CSCs treated with TCC serum displayed impaired migration and increased expression of pro-inflammatory cytokines. Cells cultured with HTP serum showed increased levels of pro-fibrotic markers, and reduced expression of connexin-43. Both TCC and HTP sera increased collagen release and reduced secretion of angiogenic protective factors from CSCs, compared to NS serum. Paracrine support to tube-formation by endothelial cells and to viability of cardiomyocytes was significantly impaired. Treatment with sera of both smokers groups impaired H_2O_2/NO release balance by CSCs and reduced early phosphorylation of several pathways compared to NS serum, leading to mTOR activation. Cotreatment with rapamycin was able to reduce mTOR phosphorylation and differentiation into aSMA-positive myofibroblasts in CSCs exposed to TCC and HTP sera. In conclusion, the circulating molecules in the serum of chronic exclusive HTP smokers induce fibrotic behavior in CSCs through activation of the mTOR pathway, and reduce their beneficial paracrine effects on endothelial cells and cardiomyocytes. These results point to a potential risk for cardiac fibrosis in chronic HTP users.

1. Introduction

Traditional tobacco combustion cigarettes (TCCs) are main risk factors for lung cancer and cardiovascular diseases. Besides the role of TCCs in the etiology and progression of endothelial damage and atherosclerosis, many studies indicate an important causal role also in triggering myocardial fibrosis. This increases the risk of atrial fibrillation and promotes maladaptive cardiac remodeling mechanisms in chronic smokers [1,2]. The main cell type responsible for fibrosis and remodeling in the heart are resident cardiac stromal cells (CSCs). These cells respond to pathological stimuli through activation from a homeostatic state, and differentiation into collagen-producing cells, that is

Abbreviations: CSCs, Cardiac stromal cells; NS, Non-smoker; TCC, Tobacco combustion cigarettes; HTPs, Heated tobacco products; MRP, Modified risk product; ECM, Extracellular matrix; NRMs, neonatal rat myocytes.

* Corresponding author at: Corso della Repubblica 79, 04100 Latina, Italy.
E-mail address: isotta.chimenti@uniroma1.it (I. Chimenti).

[1] These authors equally contributed.

https://doi.org/10.1016/j.bbadis.2024.167350
Received 18 October 2023; Received in revised form 21 June 2024; Accepted 4 July 2024
Available online 14 July 2024

myofibroblasts [3,4]. Other than direct fibrosis contribution by collagen deposition, CSCs also exert indirect effects through paracrine mechanisms on parenchymal and immune cells, as they influence cell survival and stress resistance, angiogenesis, and immune cell activation [4–6]. The use of alternative smoking devices, such as vaping electronic cigarettes and, more recently, heated tobacco products (HTPs), is increasing dramatically on a global scale [7], but their effects on human health, particularly in the long term, are still uncertain [8]. In fact, epidemiological studies on long-standing risks cannot be achieved yet, since these products are relatively new on the market. The recent SUR-VAPES-2 study [9] has showed how a single use of HTP causes an acute adverse impact on circulating markers of oxidative stress, platelet function, flow-mediated dilation, and blood pressure. These effects, though, appeared reduced compared to a single use of TCC. Interestingly, the subsequent SUR-VAPES Chronic study [10] has reported that young healthy subjects (average age 30), having exclusively used HTPs for 18 months on average, have increased oxidative stress, endothelial dysfunction, and platelet activation when compared with matched non-smokers. Most importantly, this study could not detect any differences in these parameters in comparison with matched chronic TCC smokers, suggesting a highly detrimental cardiovascular impact of HTPs. Moreover, we have recently reported a substantial effect of HTPs on the profile of circulating microRNAs in the subjects enrolled in the SUR-VAPES Chronic study [11].

Parallel to clinical research on modified risk products, many studies have assessed their molecular and biological effects on different cell types, mainly considering endothelial and lung cells [12,13]. Most of these studies, though, have been performed by direct exposure of cells to vaping e-cigarettes liquids or derived aerosols. Besides, the more recently introduced HTPs are essentially unexplored [14]. These products could exert their effects in chronic smokers likely through modification of the circulating molecular profile, which becomes particularly relevant for interstitial cell types that are not directly exposed to smoke. Thus, the biological response of myocardial cell types to circulating signals in chronic HTP smokers, and the overall molecular and cellular mechanisms of cardiovascular damage mediated by HTPs are still unknown.

We hypothesized that the significant alteration of circulating signals and increased oxidative stress caused by chronic exclusive use of HTPs can induce a pro-fibrotic phenotypic shift in resident CSCs, reducing their homeostatic properties (e.g. migration, angiogenic and trophic support) while fueling detrimental paracrine and functional features (e.g. pro-fibrotic and pro-inflammatory). To this aim, we used human atrial CSCs that can be isolated from discarded tissue of non-smoker cardiac surgery patients and exposed them to sera of patients enrolled in the SUR-VAPES Chronic clinical trial, including exclusive HTP smokers, chronic TCC smokers, and matched non-smokers (NS).

2. Methods

2.1. Human cardiac stromal cells culture

Human adult cardiac stromal cells (CSCs) were isolated from right atrial appendage tissue, as previously described [15,16], during clinically indicated procedures, after informed consent, and according to the principles of the Declaration of Helsinki, under protocol 2154/15 approved by the Ethical Committee of “Umberto I" Hospital, “La Sapienza” University of Rome. In brief, tissue was fragmented, digested, and plated as explant cultures in dishes previously coated with Fibronectin (FN) (356008, Corning) in complete explant media (CEM) formulated as follows: Iscove's modified Dulbecco's medium (IMDM) (10–016-CV, Corning) supplemented with 20 % FBS (F2442, Sigma-Aldrich), 1 % penicillin-streptomycin (P4333, Sigma-Aldrich), 1 % L-glutamine (BEB17-605E, Lonza), and 0.1 mM 2-mercaptoethanol (63689, Thermo-Fisher). Explant-derived cells were collected after 3 weeks by sequential washes with Ca^{2+}-Mg^{2+} free PBS, 0.48 mM/L Versene (15040066, Thermo-Fisher) for 3 min, and with 0.05 % trypsin-EDTA (CC-5012, Lonza) for 5 min at room temperature. Collected cells were selected for a non-differentiated phenotype by spheroid growth, as previously described [17], to deplete the culture from differentiated cells, such as myofibroblasts or smooth muscle cells; cells were then expanded as a monolayer on FN-coating in CEM. Four CSCs lines were used, obtained from donors with the following characteristics: non-smokers, free from dysmetabolic conditions (diabetes mellitus, or metabolic syndrome), under beta-blockers therapy [16,17], non-obese, non-hypertensive, with low-to-moderate cardiovascular risk scores, and not having suffered a myocardial infarction in the last 30 days (Supplemental Table 1). CSCs from different donors were always kept separate and used as individual biological replicates. For rapamycin experiments, cells were cotreated for 48 h with rapamycin 100 ng/mL (R8781, Sigma-Aldrich).

2.2. Flow cytometry

CSCs from the first explant harvest and at passage 1 were used for all donors. Cells from semi-confluent cultures were harvested with trypsin-EDTA and stained with CD90-FITC (1:500, AS02, Dianova) using 300 ng antibody in 100 μL staining buffer (PBS with 2 % FBS) per sample. All acquisitions were performed using a BD FACS-Aria II cytometer equipped with DIVA software (BD Biosciences), which was also used to calculate the compensation parameters. All flow cytometry data were analyzed with FlowJo software (FlowJo LLC).

2.3. RNA extraction and RT-qPCR

Total RNA was extracted using the miRNeasy Micro Kit (217084, Qiagen) and quantified using Nanodrop spectrophotometer (Thermo Fisher Scientific). cDNA was synthesized from 0.5 μg RNA with the High-Capacity cDNA Reverse Transcription Kit (4368814, Thermo Fisher Scientific). Real-time qPCR was performed to assess gene expression using Power SYBR Green PCR Master Mix (4368577, Thermo Fisher Scientific) and standard thermocycling conditions, according to the manufacturer's protocol. The relative ratio versus reference gene was calculated using the comparative Ct method ($2^{(-\Delta Ct)}$). The set of genes analyzed, and the primers sequences are listed in Supplemental Table 2. Hypoxanthine Phosphoribosyltransferase 1 (HPRT1) was selected as the best housekeeping gene according to the Bestkeeper spreadsheet macro (freely available at: www.gene-quantification.de). The PCR data was analyzed ($2^{(-\Delta Ct)}$ for the retrospective analysis, or fold change versus NS for the in vitro treatments), and Volcano Plots were generated by multiple *t*-test analysis using GraphPad Prism 8 software (GraphPad Software).

2.4. Spheroid assay

For the spheroid forming assay, $1{,}5 \times 10^4$ CSCs per well were plated in 24-well plates coated with Poly-D-Lysine (354210, Corning), in CEM supplemented with 10 % human serum from the NS, TCC, or HTP lots. Whole well images were captured after 7 days of culture with a Nikon Eclipse Ti microscope equipped with NIS-Elements AR 4.30.02 software (Nikon Corporation). Images were analyzed using ImageJ software exploiting the plugins for particle counts and area measurement.

2.5. Immunostaining and fluorescence microscopy analysis

Cells were fixed for 10 min with 4 % paraformaldehyde at 4 °C, and permeabilized with 0.1 % Triton X-100 (11332481001, Sigma-Aldrich) in PBS with 1 % BSA. Nonspecific antibody binding sites were blocked with 10 % FBS (Sigma-Aldrich) in PBS, before overnight incubation at 4 °C with primary antibody anti-CX43 (1:50, MAB306, Millipore) and anti-αSMA (1:50, A2547, MERK). After thorough washing, slides were incubated for 2 h at room temperature with Alexa-Flour 488 secondary antibody (1:500, A-11001, Thermo-Fisher) and Hoechst nuclear dye

(1:10000, H3570, Thermo-Fisher). Slides were mounted in Vectashield (H-1000-10, VectorLabs). Image capture was performed on a Nikon Eclipse Ni microscope equipped with VICO system, and average fluorescence intensity per cell area was calculated by semi-automatic methods using NIS-Elements AR 4.30.02 software with a 20× objective (Nikon Corporation).

2.6. Soluble collagen assay

CSCs were treated for 48 h with CEM supplemented with 10 % human serum derived from NS, TCC, or HTP serum lots. Then, conditioned media was collected after 24 h, and soluble collagen was quantified using Sircol Soluble Collagen Assay (S1000, Biocolor), according to the manufacturer's instructions. The absorbance at 590 nm was recorded using Varioskan™ LUX Multimode Reader (Thermo Fisher Scientific). Data was analyzed using the Skanlt software (Thermo Fisher Scientific).

2.7. Scratch assay

CSCs (10^5 per well) were plated in 12-well plates coated with Fibronectin (356008, Corning) in CEM 10 % FBS. The scratch was performed after 24 h from plating: cells were washed with PBS and then cultured with CEM supplemented with 10 % human serum derived from NS, TCC, or HTP serum lots. Images were captured after 6, 8 and 10 h with a Nikon Eclipse Ti fluorescence microscope, equipped with motorized stage and NIS-Elements AR 4.30.02 software (Nikon Corporation). Images were analyzed by ImageJ software using an automatic macro for scratch area measurement.

2.8. Cytokine array for secretome profiling

CSCs were pre-treated for 48 h with media supplemented with 10 % human serum derived from NS, TCC, or HTP serum lots. After thorough washing, cells were cultured for the following 24 h with CEM 0,1 % FBS for conditioned media (CM) collection. Media were gently aspirated and centrifuged at 2000 rcf for 5 min to remove cells and debris, and then stored at −80 °C until analysis. Media were assayed using the Proteome Profiler Human XL Cytokine Array (ARY005B, R&D Systems), according to the manufacturer's instructions. Optical density (OD) of membranes was quantified by the ChemiDocXRS+ Imager (Bio-Rad), and densitometric analysis was performed using Image Lab software (Bio-Rad). The data obtained (log2-trasformed densitometric quantification of each dot) was plotted as a heatmap generated using the pheatmap R package (GNU Project). Functional association network was created using the STRING database (ELIXIR Core Data Resources) selecting the "experiments" and "database" as interaction sources, and high confidence (0.70) as the minimum interaction score.

2.9. Assays on conditioned media

Adiponectin concentration was evaluated using the specific ELISA kit (EK0595, Boster) following the manufacturer's protocol. Absorbance at 450 nm was recorded immediately after the end of all steps using the Varioskan Lux multimode microplate reader (Thermo Fisher Scientific). The data were analyzed using the Skanlt software (Thermo Fisher Scientific). H_2O_2 and NO release were measured by Colorimetric Detection Kits (K034—H1 and K023—H1, respectively; Arbor Assays), and values were expressed as μmol/L.

2.10. Angiogenesis assay

The tube forming assay was performed as previously described [18], with human umbilical vein endothelial cells (HUVECs) routinely cultured with standard protocols in EGM2 media (CC-4176, Lonza). Cells were plated $1{,}5 \times 10^4$ per well for 16 h on matrigel-coated 96-well plates (Growth Factor Reduced Matrigel Matrix Phenol Red Free, 356234, BD) in presence of the CSC-CMs collected in CEM 0.1 % FBS. An automated scan of each well was acquired with a 4× objective by Nikon Eclipse TI inverted microscope with motorized stage (Nikon Corporation). Quantification of the number of nodes, number of master segments, number of meshes, and mesh area were performed by ImageJ software and the Angiogenesis plugin (NIH).

2.11. MTS cardiomyocyte viability assay

MTS cell viability assay was performed to evaluate neonatal rat myocytes (NRMs) viability using Cell Titer 96® Aqueous Non-Radioactive Cell Proliferation Assay (MTS) (G5421, Promega). NRMs were isolated from 2 day-old Sprague Dawley rat pups by the Neonatal Cardiomyocyte Isolation Kit, on a gentleMACS Dissociator (130–100-825, Miltenyi Biotec), according to the manufacturer's protocols. NRMs were plated in 96-well plates (1 × 10^3 per well) in 100 μL Cardio Medium DMEM/F-12 (D0547, Sigma-Aldrich) supplemented with 0.72 g/L glucose (G5400, Sigma-Aldrich), 0,33 g/L sodium pyruvate (BP356, Thermo Fisher Scientific), 0.017 g/L ascorbic acid (13080–23, Gibco), 2 μL selenite 0.2 M (S5261, Sigma-Aldrich), 0.004 g/L transferrin (T3309, Sigma-Aldrich), 2 g/L BSA fraction V (0332, VWR), 3.57 g/L HEPES (0511, VWR), 2.43 g/L sodium bicarbonate (S6014, Sigma-Aldrich) and 10 mL penicillin-streptomycin (15070063, Gibco). After 24 h, NRMs were incubated with conditioned media, or Cardio Medium as the positive experimental control. NRMs viability was measured 48 h after treatment adding 20 μL of combined MTS/PMS Solution to each well containing cells in 100 μL of medium, and incubating for 2 h. The absorbance at 490 nm was recorded using Varioskan™ LUX Multimode Reader (Thermo Fisher Scientific). The data were analyzed using the Skanlt software (Thermo Fisher Scientific).

2.12. Human phospho-kinase array

CSCs were serum-starved for 4 h, and then treated for 1 h with CEM supplemented with 10 % human serum derived from NS, TCC, or HTP serum lots. After thorough washing, cells were collected, total protein was isolated with Ripa buffer (89900, Thermo-Fisher) and quantified with DC Protein assay (23200, Bio-Rad). 400 μg of proteins were assayed using the Proteome Profile Human Phospho-Kinase array kit (ARY003C, R&D Systems), according to the manufacturer's instructions. Optical density (OD) of membranes was quantified by the ChemiDocXRS+ Imager (Bio-Rad), densitometric analysis was performed using Image Lab software (Bio-Rad), and a heatmap of normalized OD values was created by pheatmap R package (GNU Project).

2.13. Western blot

Total cell proteins were isolated using Ripa buffer (89900, Thermo Fisher) and stored at −80 °C until analysis. Equal volumes of protein lysate were loaded on sodium dodecyl sulfate 8 % or 12 % polyacrylamide gel for electrophoresis (SDS-PAGE) and transferred to PVDF membranes (GE10600069, Sigma-Aldrich). Membranes were then blocked with 3% BSA or 5% MILK for 1 h at room temperature, and incubated with primary antibodies against mTOR, p-mTOR, AKT, p-AKT and Vinculin (dilution 1:100 for all; catalog 2972, 2971, 9272, 9271 and 4650, Cell Signaling Technologies) at 4 °C overnight under gentle agitation. Membranes were then washed with TBS-0.1 % Tween, and incubated with HRP-conjugated secondary antibodies (5104–2404, Bio-Rad) for 1 h, before detection with Clarity western ECL (1705061, Bio-Rad). The chemiluminescence signal was detected by ChemiDoc XRS+ and densitometric analysis was performed using ImageLab software (all Bio-Rad). The relative band abundance was normalized versus Vinculin, as the loading control.

2.14. Statistical analysis

For clinical record analyses, variables are reported as median (1st; 3rd quartile) for continuous variables, and count/total (percentage) for categorical variables. Differences were computed with unpaired Mann-Whitney *U* test for continuous variables, and Fisher exact test for categorical variables using SPSS (IBM, version 25, USA). Significance was set at <0.05. For experimental data, results are presented as mean value ±SEM, unless specified. For in vitro treatment results, inter-patient variability was controlled for by normalizing experimental results of each CSC line versus the NS control, and averaging fold-change modulations. Datasets were checked for significant outliers by Prism 8 software (GraphPad Software), which were excluded when present. Normality of data was assessed and significance of differences among groups was determined by one-way ANOVA, with Bonferroni or Fisher LSD post-test, as appropriate, using Prism 8 (GraphPad Software). A *p*-value <0.05 was considered significant.

3. Results

3.1. Human CSC isolation and characterization

Since the features of CSCs derived from chronic TCC smokers had never been described, as a preliminary step we retrospectively analyzed experimental data of resident CSCs previously isolated in our lab from patients undergoing elective cardiac surgery [17]. An overall flow cytometry and immunofluorescence profile of CSCs at basal conditions is provided in Supplemental Fig. 1A and B, respectively. We stratified samples as non-smoker donors (never smoked, 20 CSC lines), and smoker donors (former or current, 18 CSC lines). Available cell culture, flow cytometry, and gene expression data were evaluated. The analysis evidenced: a significant impairment in the mesenchymal/stromal capacity of spontaneous 3D growth (Supplemental Fig. 1C); a significant increase in the percentage of cells positive for the pro-fibrotic marker CD90 (Supplemental Fig. 1D); significantly higher levels of the myofibroblast markers *ACTA2*, and of the oxidative stress enzymes *NOX2* and *NOX5* in CSCs derived from smokers compared to non-smoker donors (Supplemental Fig. 1E). Thus, to exclude biases due to fibrotic commitment of CSCs at basal conditions, we selected for all further experiments CSCs isolated from non-smokers, undergoing beta-blocker therapy [16], and free from diagnosis of dysmetabolic conditions (metabolic syndrome, or type 2 diabetes) [17].

3.2. Human serum lot creation

Human serum had been collected previously from young healthy non-smokers (NS), chronic exclusive HTP smokers (mean exclusive use of 1.5 ± 0.5 years), and chronic TCC smokers (mean exclusive use of 7 years), enrolled in the SUR-VAPES Chronic study as three highly homogeneous cohorts [10] (Supplemental Table 3). Blood collection was performed at 8.00 a.m. after an 8-h abstinence period from smoking. Due to the limited volumes available, identical volumes of serum from the 20 homogeneous patients per group were pooled to create three representative serum lots used in all following experiments with CSC cultures. Each of the 4 CSC lines was then cultured up to 48 h in media supplemented with 10 % serum lot of either NS, HTP or TCC smokers.

3.3. Cell phenotype after treatment with serum from exclusive HTP smokers

The spontaneous capacity to grow in 3D was quantified, as a feature of mesenchymal phenotype [19,20]. The number of spheroids formed by plating the same cell number significantly decreased when CSCs were cultured in the TCC versus the NS serum lot, (Supplemental Fig. 2A-B), and with comparable spheroid size among groups (Supplemental Fig. 2C). This result suggests a possible reduction in a typical stromal feature in treated CSCs.

Supplemental Fig. 2D shows the percentage of cells positive for the fibrosis marker CD90 by flow cytometry in CSCs cultured with the different serum lots.

Next, we analyzed the differential capacity of the three serum lots to stimulate migration in CSCs. We observed a significantly higher residual scratch area after 6 h for cells treated with the TCC serum lot versus the NS lot (Fig. 1A-B). Cells cultured with the HTP serum lot showed an intermediate migration ability. A significantly higher residual area in CSCs exposed to the TCC serum lot was maintained up to 10 h, instead the effect on migration of the HTP serum gradually aligned with that of the NS control (Fig. 1C-D). This suggests that serum from chronic TCC smokers has a reduced capacity of sustaining stromal cells migration, while that of HTP smokers exerts a midway effect between NS and TCC.

The gene expression profile of CSCs exposed for 48 h to treatment with the 3 serum lots is presented in Fig. 2A. This analysis evidenced a significant up-regulation of the pro-inflammatory cytokines *IL6* and *IL8* in CSCs exposed to the TCC serum lot versus the NS lot (Fig. 2A), as well as a significant up-regulation of the extra-cellular matrix (ECM) remodeling marker *MMP1*, of the fibroblast activating cytokine *PDGFA*, and of the oxidative stress enzyme *NOX5*. We also detected a significant downregulation of type III collagen (*COL3A1*) and *NOX4* in cells treated with the TCC serum lot compared to the NS control (Fig. 2A). On the other side, CSCs treated with the HTP serum lot displayed significant upregulation of type I collagen (*COL1A1*), *THY1* (encoding for CD90), *PDGFA*, and the oxidative stress enzyme *NOX2*, all versus treatment with the NS lot (Fig. 2B). *ACTA2* expression was upregulated on average >10-fold, albeit not reaching statistical significance. Conversely, *VEGFA, GJA1* (encoding for connexin-43), and *MMP1* were significantly downregulated after culture with the HTP serum lot compared to the NS control (Fig. 2B). When evaluating gene expression levels between TCC and HTP serum lot treatments (Supplemental Fig. 3), results showed significantly higher levels of *IL6*, *IL8*, *VEGFA* and *MMP1,* and significantly lower levels of *COL1A1* in CSCs cultured with the TCC serum lot versus the HTP lot.

The importance of cardiac stromal cells in the electrical conductance of the heart has recently emerged. Connexin-43 is expressed in fibroblasts as a mediator of their electrical integration, and in these cells it can be sufficient to conduct the electrical stimuli, for example through the scar tissue [21], or to recapitulate physiopathological features of arrhythmias [22]. Atrial fibrillation has been associated with reduced connexin-43 expression [23,24], increased myofibrillar protein expression in fibroblasts, and increased deposition of ECM [25]. First, we assessed connexin-43 expression by immunofluorescence staining, and detected a significant reduction in the average fluorescence intensity per cell area in CSCs treated with the HTP serum lot, compared to both NS and TCC lots (Fig. 2C-D), consistently with the gene expression modulation (Fig. 2B). Moreover, immunofluorescence intensity of the main myofibroblast activation marker, that is alpha-smooth muscle actin (αSMA), was significantly increased in both smokers' sera groups (Fig. 2E-F), with enhanced fibrillar profiles (Supplemental Fig. 4). Increased extracellular release of soluble collagen (Fig. 2G) was also detected in HTP and TCC treatment groups, all compared with NS sera.

3.4. Paracrine profile after treatment with serum from exclusive HTP smokers

We analyzed the profile of cytokines present in the cell culture medium supplemented with 10 % human sera before use, as well as after 48 h of culture, and after additional 24 h of culture in human serum-free media (see Fig. 3A for experimental design). In particular, these latter samples (dubbed "CM 48 h + 24 h") were collected after removal of human serum-supplemented media and its replacement with 0.1 % FBS-IMDM, which was then conditioned for additional 24 h. Thus, these latter conditioned media contained only molecules released by CSCs. All conditioned media were screened by protein arrays, and log2 optical

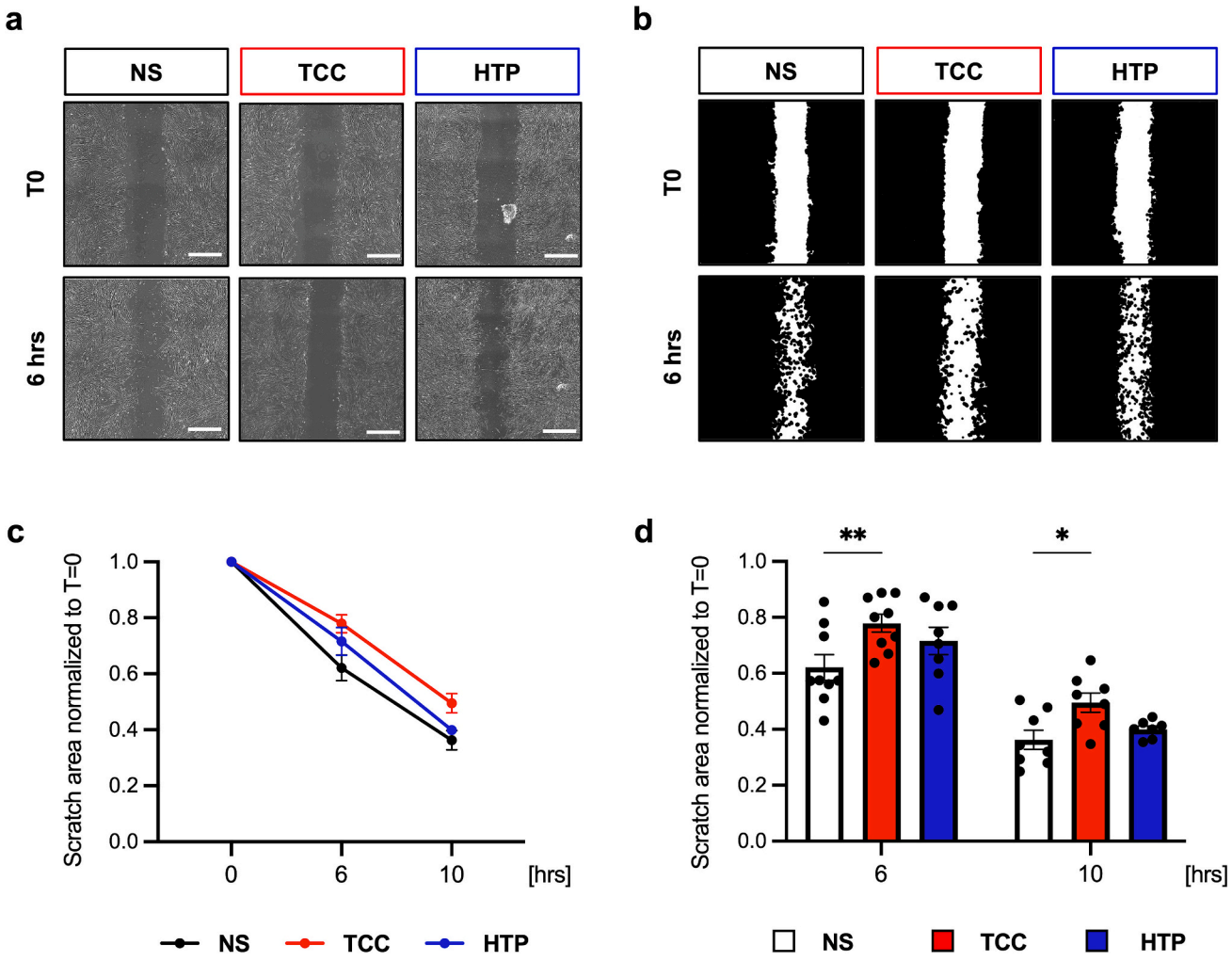

Fig. 1. CSC migration capacity in response to serum lots of smokers. Representative bright field microscopy images (a) and relative binary masks obtained by the ImageJ macro (b) of the residual area of the scratch assay performed with CSCs (each in experimental triplicate) cultured in serum lots from non-smokers (NS), tobacco combustion cigarette (TCC), or heated tobacco product (HTP) smokers. The quantification of the residual surface area is plotted as normalized values in time (c), as well as dot plots bar graph for each single time-point (d). $N = 9$ (3 experimental replicates for 3 CSC lines). * $P < 0.05$, ** $P < 0.01$. Scale bar = 500 μm.

density (OD) values were plotted as heatmap (Fig. 3B). Hierarchical clustering allowed us to identify a specific cluster of molecules enriched only in human sera-free media, thus actively produced and released by CSCs because of the conditioning with the serum of TCC, HTP or NS subjects. When analyzing this specific cluster, differences emerged between the 3 groups (Fig. 3C, Supplemental Table 4). For example, media from CSCs treated with sera of both smokers type had lower levels of protective molecules (e.g. VEGF, Adiponectin, CHI3L1, GDF-15) compared to NS serum treatment, while the TCC sample was enriched in many pro-inflammatory molecules (e.g. IL-6, IL-8, PTX3, SDF-1, CD40L, MIF). This shortlist of cytokines was loaded on the STRING database for network analysis, and the resulting network (showing connections with interaction score >0.4) confirmed the strict relations among many of them (Fig. 3D). The Gene Ontology analysis on the STRING database returned a long list of significant terms involved. A selection of GO terms with high strength (>1, meaning >10-fold enrichment) and highly significant false discovery rate (FDR) is reported in Supplemental Table 5, including several terms of cardiovascular diseases: "Artery disease" (DOID:0050828), "Atherosclerosis" (DOID:1936), "Myocardial infarction" (DOID:5844). We validated the protein array by confirming significantly reduced concentration of secreted adiponectin by ELISA (Fig. 3E) in the supernatant of cells previously treated with both HTP and TCC serum lots versus NS serum-treated cells, and consistently modulated transcriptional levels for *CHI3L1*, *IL6*, and *IL8* (Fig. 3F-H).

Additionally, we quantified the release of H_2O_2 and NO in the conditioned media, as indicators of the balance between oxidative stress and pro-angiogenic properties. We detected a significantly higher concentration of H_2O_2 in conditioned media from cells pre-treated with the TCC serum lot versus the NS lot (Fig. 3I), and a significant reduction in NO concentration released by CSCs pre-treated with TCC and HTP serum lots, both compared to the NS control (Fig. 3J). Notably, H_2O_2 release was higher from cells previously cultured in the HTP serum lot compared to the NS control, albeit to a significantly lower concentration compared to CSCs treated with the TCC lot.

3.5. *Functional paracrine features after treatment with serum from exclusive HTP smokers*

We then assessed the paracrine effects of CSC-conditioned media (human-serum free) concerning support to endothelial cells for angiogenesis, and to cardiomyocytes for cell viability. The angiogenic assay on Matrigel with HUVECs evidenced a significant reduction in the pro-angiogenic features of conditioned media from cells pre-treated with both TCC and HTP serum lots, compared to the NS lot (Fig. 4A). Several indexes were evaluated, including number of nodes, master segments and meshes, and the total mesh area (Fig. 4B). The same conditioned media were also used to culture neonatal rat myocytes (NRMs) under

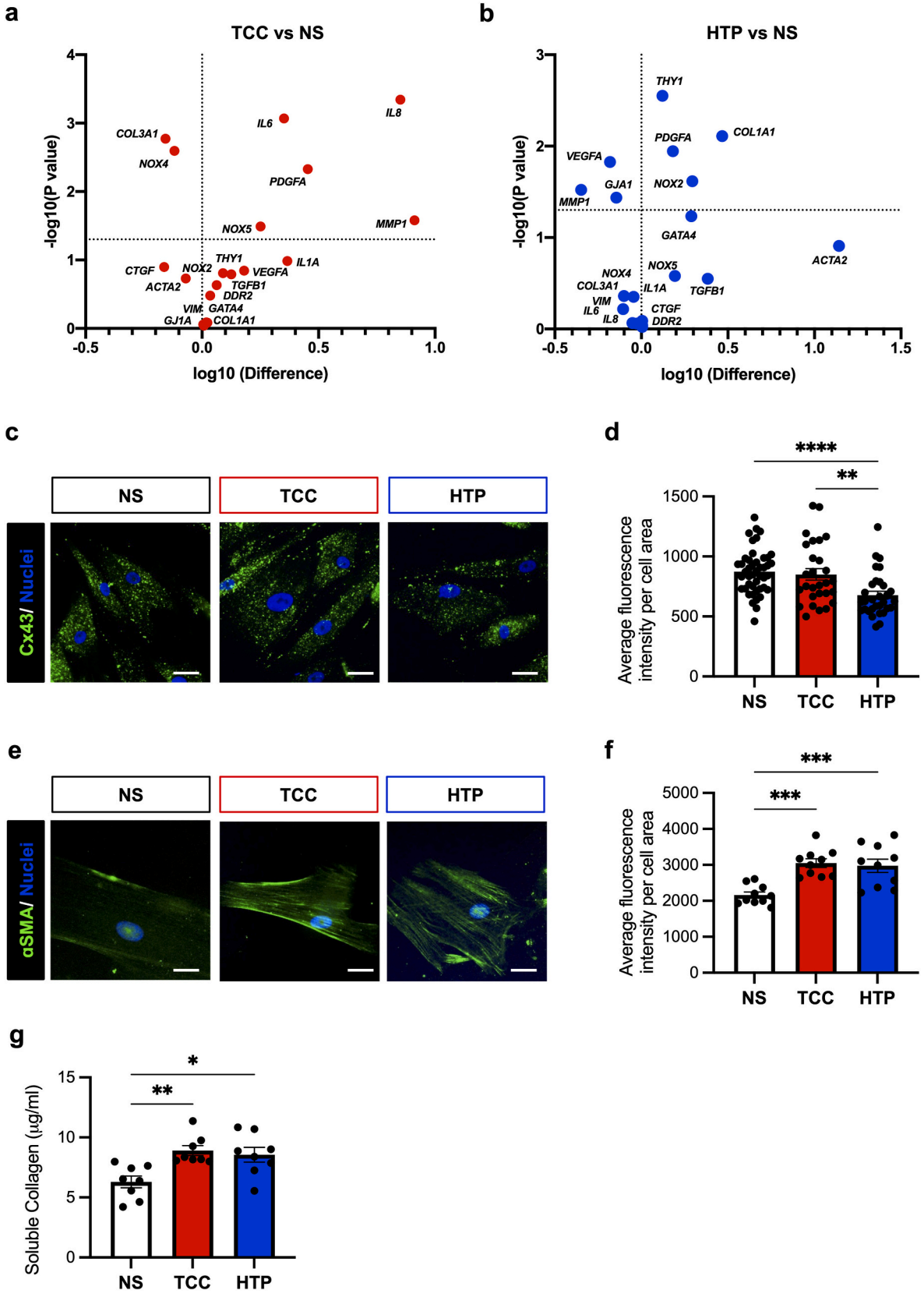

Fig. 2. Gene expression profiles of CSCs after treatment with serum lots of smokers. The relative gene expression levels by realtime PCR, with corresponding significance values, are plotted as volcano plot for the comparison of tobacco combustion cigarette (TCC)- versus non-smoker (NS)-serum lot treatments of CSCs (a), and of heated tobacco product (HTP)- versus NS-serum lot treatments (b). $N = 3$ (3 CSC lines for each of the 3 serum lots). Representative immunofluorescence panels (c), and quantification of average fluorescence intensity per cell area (d) of connexin-43 (Cx43) and alpha-smooth muscle actin (αSMA) (e-f) after 48 h of culture of CSCs in the different serum lots. N (analyzed cells per condition) ≥28. Scale bar = 50 μm. g) Quantification of soluble collagen concentration by Sirius Red assay, released in conditioned media by CSCs after 48 h. * $P < 0.05$, ** $P < 0.01$, *** $P < 0.001$, **** $P < 0.001$.

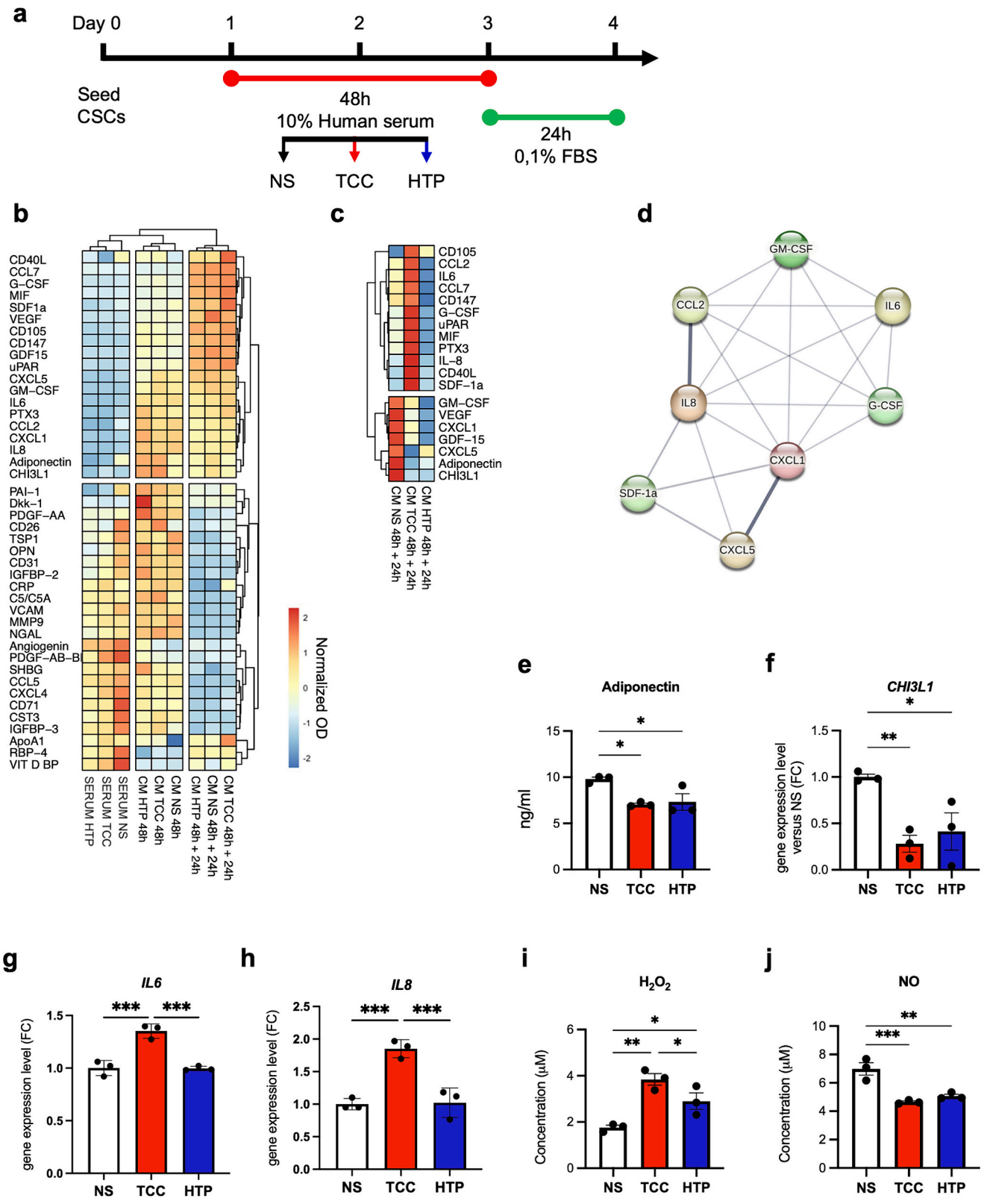

Fig. 3. Profile of molecules secreted by CSCs after treatment with serum lots of smokers. Fresh media with 10 % human sera, conditioned media after 48 h of culture (CM 48 h), and conditioned media (without human serum) after additional 24 h (CM 48 h + 24 h) were collected from CSCs treated with the serum lots from non-smokers (NS), tobacco combustion cigarette (TCC), or heated tobacco product (HTP) smokers (a). All CMs were screened by protein arrays and Log2 optical density (OD) values were then plotted as heatmap with hierarchical clustering (b). The upper cluster corresponding to molecules enriched only in human serum-free media (CM 48 h + 24 h) were further analyzed by heatmap and clustering (c), and the corresponding network of functional associations was obtained from the STRING database (d). Validation of the protein arrays was performed by ELISA for adiponectin (e), and by RT-qPCR for *CHI3L1* (f), *IL6* (g), and *IL8* (h). The concentrations of hydrogen peroxide (H_2O_2) (i) and nitric oxide (NO) (j) were also analyzed in the human serum-free conditioned media (CM 48 h + 24 h). N = 3 (3 CSC lines for each of the 3 serum lots). * $P < 0.05$, ** $P < 0.01$, *** $P < 0.001$.

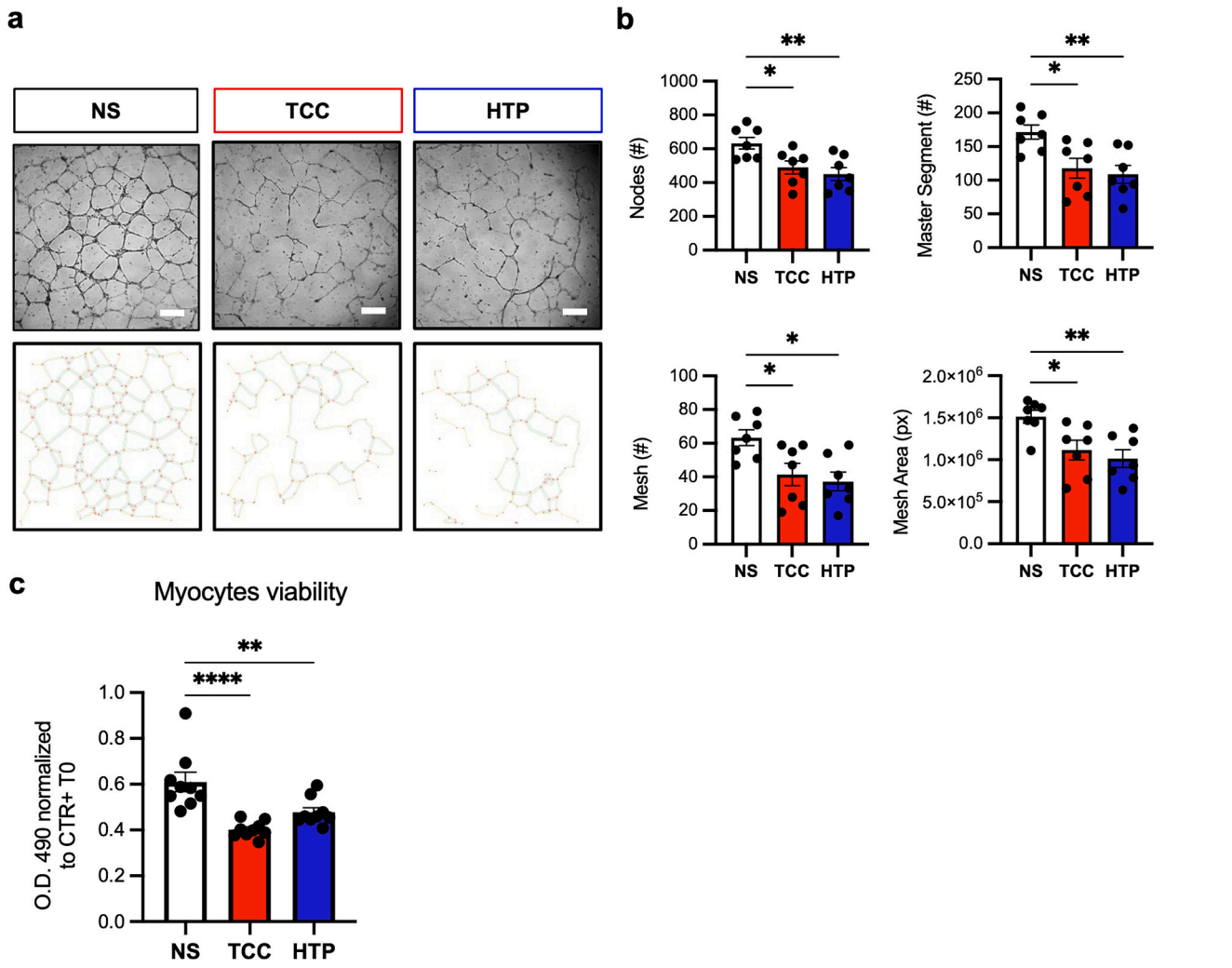

Fig. 4. Functional paracrine effects of CSC conditioned media on endothelial cells and cardiomyocytes. Human umbilical vein endothelial cells (HUVECs) were cultured overnight on Matrigel with human serum-free media conditioned by CSCs previously treated with serum lots from non-smokers (NS), tobacco combustion cigarette (TCC), or heated tobacco product (HTP) smokers. Representative images of cultures are shown (a), with quantification of the number of nodes, master segments, meshes, and the mesh area (b) in the different conditions. $N = 7$ (at least 2 experimental replicates for each conditioned media derived from 3 CSC lines). Neonatal rat myocytes (NRMs) were cultured for 48 h with media previously conditioned by CSCs (each in experimental triplicate), and in cardio-medium as the experimental control (CTR+). Optical Density (OD) values normalized to that of T0 of culture are shown for the different conditions (c). N = 9 (3 experimental replicates for each conditioned media derived from 3 CSC lines). * $P < 0.05$, ** $P < 0.01$, *** $P < 0.001$, # $P < 0.0001$. Scale bar = 200 μm.

starvation (0.1 % FBS in IMDM), and their viability was monitored by MTS assay. Compared to the positive experimental control, media conditioned by CSCs previously exposed to the NS serum lot was able to significantly reduce cell death in the first 48 h of culture, compared to media conditioned by cells exposed to both TCC and HTP serum lots (Fig. 4C). Overall, this data indicates a detrimental effect of circulating molecules in TCC and HTP smokers on the protective paracrine functions of CSCs, albeit to a different extent for some features concerning HTP smokers.

3.6. Signal transduction pathways activation after treatment with serum lots and involvement of the mTOR pathway

TCC and HTP serum lots contain significantly increased levels of ROS [10]. Increased oxidative stress has been reported to promote dephosphorylation of multiple transduction proteins [26–28]. Therefore, we hypothesized that impaired upstream phosphorylation pathways may be involved in the cell phenotypes observed in our setup. We screened the differential activation of transduction pathways in CSCs by phospho-protein array after treatment with TCC and HTP serum lots for 1 h. We detected reduced phosphorylation of multiple proteins (Fig. 5A), including p38, STAT3/5, GSK-3a/b, p53, AKT, PRAS40, and CREB. Among the modulated proteins in the array, Akt, PRAS40, GSK3a/b, and p53 share one common target, that is mTOR (Fig. 5B), which is a key protein involved in fibrosis and cardiovascular diseases [29–34]. Therefore, we analyzed the mTOR pathway by WB after 48 h of culture in each serum lot. Analysis showed significantly increased phosphorylation of mTOR (Fig. 5C-D) after exposure to HTP and TCC serum lots, compared to NS. We obtained the specific inhibition of mTOR phosphorylation by concurrent treatment with rapamycin during TCC, HTP or NS serum lot treatments of CSCs (Fig. 5C-D). Rapamycin coherently induced increased upstream Akt phosphorylation (Fig. 5C-E) [35]. Consistently, rapamycin cotreatment caused the reduction of CSC activation and myofibroblast differentiation when exposed to TCC and HTP serum lots, as detected by significantly reduced αSMA fluorescence intensity and polymerization compared to control NS serum lot (Fig. 5E-F).

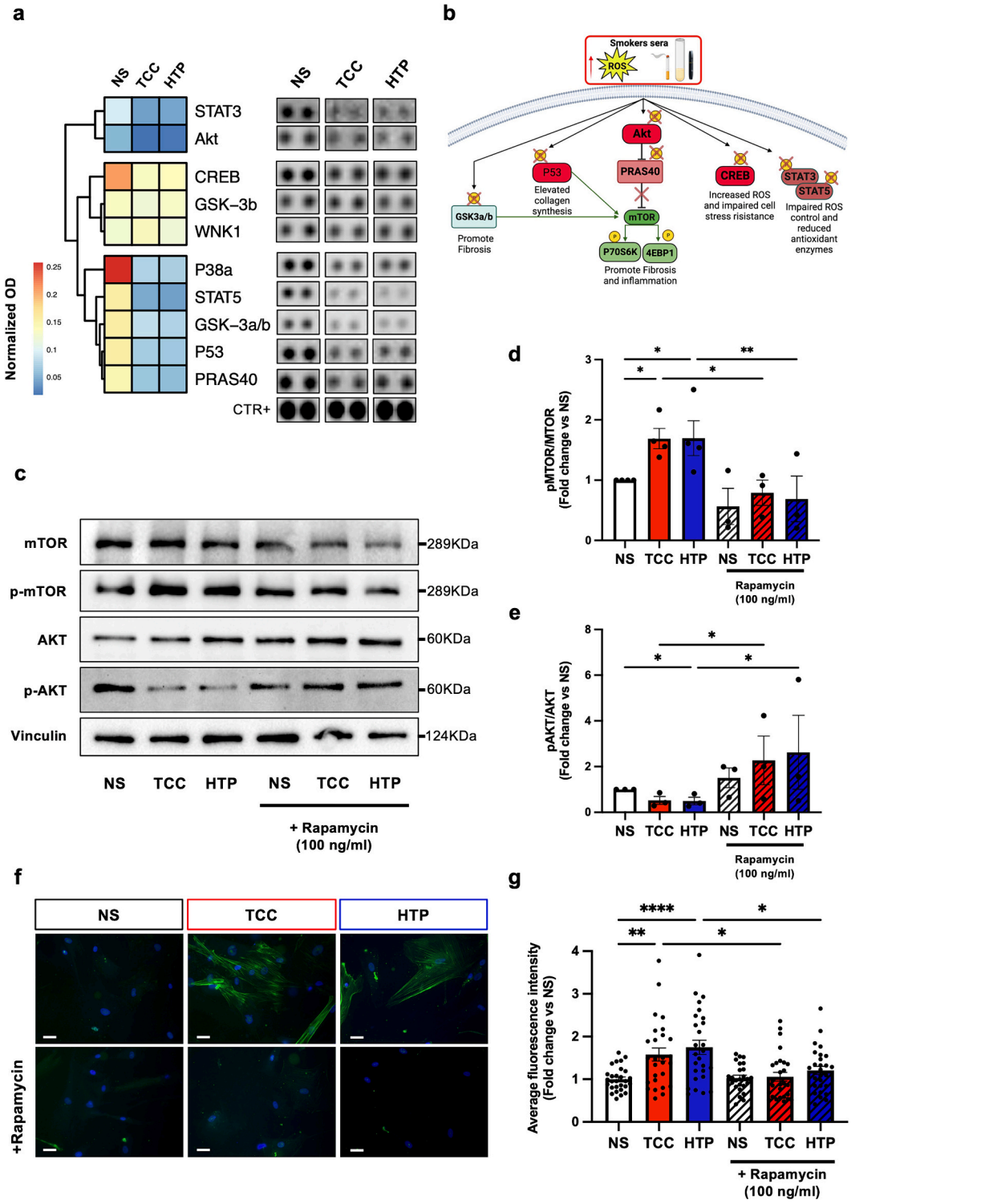

Fig. 5. Signal transduction pathways and involvement of mTOR in CSCs response to serum lots of smokers. (a) Representative blots of the Phospho-protein array on CSC protein lysates after exposure for 1 h to serum lots from non-smokers (NS), tobacco combustion cigarette (TCC) or heated tobacco product (HTP) smokers; normalized OD values were used to create the corresponding clustered heatmap. Schematic representation of the interactions among ROS, fibrotic pathways, and phosphorylation profiles of the different pathways screened by phospho-array and WB (b). Representative western blot panels (c) and densitometric analysis (d-e) for phosphorylated mTOR and AKT after 48 h of NS, TCC and HTP sera treatments, with or without cotreatment with rapamycin. $N = 4$ (CSC lines for each of the 3 serum lots). Representative immunofluorescence panels (f) and quantification of average fluorescence intensity per cell area (g) of alpha-smooth muscle actin (αSMA) after 48 h of culture of CSCs in the different serum lots, with or without rapamycin cotreatment. N (analyzed cells per condition) ≥28. * $P < 0.05$, ** $P < 0.01$, **** $P < 0.001$. Scale bar = 25 μm.

4. Discussion

Tobacco combustion cigarette (TCC) smoking represents a major lifestyle risk factor for cardiovascular diseases, which accounts approximately for 25 % of cardiovascular deaths [36] The use of novel smoking devices is increasing rapidly worldwide. As of 2018, an estimate of 2.4 % among the adult population in the US had used heated tobacco products (HTPs) (source: www.cdc.gov). This proportion appears even higher in the European Union, where HTPs have been introduced on the market earlier, with estimates of 6.5 % of adults who had used HTPs in 2021 [37]. These numbers are destined to increase, as more and more people appear to start using HTPs, alone or in combination with TCCs. Thus, unveiling the exact mechanisms and extent of cardiovascular damage due to chronic HTP use is of paramount importance to understand and define their prospective impact on health. Many molecular and cellular mechanisms responsible for detrimental cardiovascular effects have been described for TCCs, but there is a significant gap in knowledge about the mechanisms and damage extent related to chronic use of HTPs.

The patients recruited in the SUR-VAPES Chronic trial as exclusive HTP chronic smokers represent a one-of-a-kind cohort [10]. By using this unique collection of smokers' serum, we have provided data on how human atrial CSCs can be activated by the circulating molecular fingerprint and increased oxidative stress imposed by chronic HTP smoke [10,11]. Our results contribute unprecedented insights on how the myocardial microenvironment may be changed due to chronic HTP use. Moreover, the present study provides the first basis for a realistic definition of the potential cardiac insult caused at the cellular level by chronic use of these novel smoking devices. Importantly, our results are obtained on primary atrial resident CSCs, that is a cell population directly involved in atrial fibrosis, which is the main known mechanism involved in the development of atrial fibrillation in chronic TCC smokers [1].

Results have shown how the HTP serum lot appeared to elicit similar effects to the NS serum lot, but different from the TCC lot, considering the increase in profibrotic CD90+ cells with time in culture, trophic support, or the stimulation of migration. Conversely, the serum from HTP smokers appeared to directly modulate the mRNA levels of markers of fibroblast activation and differentiation (e.g. *COL1A1*, *THY1*, *ACTA2*) and of potential contribution to arrhythmias (*GJA1*). In fact, the HTP lot was the only one able to significantly reduce both mRNA and protein levels of *GJ1A*/Cx43 in our conditions, consistently with a pro-fibrotic and pro-arrhythmogenic shift of the stromal population. Conversely, the serum of TCC smokers was the only one capable of inducing the modulation of pro-inflammatory genes (e.g. *IL6*, *IL8*). In this regard, both TCC and HTP sera induce pro-fibrotic features, as suggested by similar increased expression of αSMA and extracellular collagen release, but the one from TCC smokers appears to induce a more evident pro-inflammatory profile, possibly linked to a reduced trophic support and to even stronger pathogenetic drive.

The difference between TCC and HTP serum lots was also evident in the profiles of secreted factors by CSCs, where exposure to the serum of TCC smokers was specifically associated to higher release of many immune activating cytokines by CSCs. Nonetheless, the secreted levels of many protective molecules (e.g. adiponectin, NO, CHI3L1) were similarly reduced in CSC-conditioned media after exposure to both HTP and TCC serum lots, compared to NS control. Interestingly, the impairment of in vitro paracrine support to endothelial cells from CSC conditioned media appeared similar after treatment with both HTP and TCC sera, compared to NS control. This was consistent with NO release levels, although VEGF mRNA and protein levels appeared significantly reduced only with treatment of the HTP serum lot in our conditions. Conversely, the paracrine pro-survival support to cardiomyocytes under stress appeared more compromised in CSCs exposed to the TCC serum lot, while treatment with the HTP lot performed in between the TCC and NS groups. These results recall studies reporting worst prognosis after myocardial infarction in smokers, associated with enhanced acute inflammation and higher incidence of infarct zone hemorrhage [38]. Overall, data point to the reduction of cardioprotective paracrine effects in vitro by the cardiac stroma due to the circulating molecules in the serum of chronic HTP smokers.

Based on our phospho-protein screening and the literature, increased circulating levels of ROS could play a key part in blunting several pathways in our system. In fact, we describe reduced levels of several phosphorylated proteins in CSCs exposed to HTP sera. Specifically, ROS can directly drive Akt de-phosphorylation [26,28], and thus negatively impact the activity of PRAS40, P53, and GSK3. These proteins have an antifibrotic function [39,40], and inhibit mTOR activity in homeostatic conditions [30,32,41]. Consistently, ROS and other circulating molecules present at higher concentrations in both TCC and HTP sera are associated to the de-phosphorylation of Akt, p53, and GSK3, directly or indirectly activating the mTOR pathway and inducing a pro-fibrotic activation in CSCs. Coherently, we have also observed strong de-phosphorylation of CREB, STAT3, and STAT5 proteins which are involved in ROS control and antioxidant enzymes production [42,43]. We have also described the direct role of mTOR phosphorylation in the fibrotic activation of CSCs after exposure to TCC and HTP serum lots. In summary, our findings suggest that increased circulating oxidative stress in chronic HTP smokers may have a significant impact on intracellular signaling pathways leading to enhanced mTOR pathway activation, with consequent profibrotic behavior and reduced beneficial paracrine effects of human atrial CSCs.

To the best of our knowledge, only one study so far had investigated the effects of human serum derived from modified risk product smokers on the phenotype of cells of cardiovascular interest, focusing on human induced pluripotent stem cell-derived endothelial cells [44]. The authors reported using mixed sera of two vaping e-cigarette smokers with those of two dual e-cigarette/TCC smokers, comparing this mixed pool with sera of TCC smokers that were 10 years older, on average. Thus, the investigation on sera from HTP smokers has never been performed previously. Moreover, the serum lots obtained from the SUR-VAPES Chronic trial used in the present report correspond to a unique homogenous cohort of 60 matched subjects, among which the HTP group included only exclusive chronic HTP smokers, thus strengthening the reproducibility and significance of our results.

One limitation of our study concerns the low number of CSC lines used, due to the multiple exclusion criteria that had to be considered for donor selection based on parameters already known to affect the fibrotic features of isolated CSCs (i.e. dysmetabolic conditions, beta-blockers therapy, tobacco smoking). Nonetheless, we have studied the response of primary human CSCs freshly isolated from the atrial tissue of clinically relevant donors. Another limitation relies in the mismatched age between cell and serum donors, but this cannot be overcome given the anthropometric differences in the patient profiles between the exclusive HTP users enrolled in the SUR-VAPES Chronic trial, and the patients undergoing elective cardiac surgery that can be enrolled as cell donors. On a different perspective, the use of serum from young healthy cohorts of matched donors reduces the risk of bias due to potential confounding variables, such as comorbidities or aging.

5. Conclusions

In conclusion, we provide data supporting for the first time the potential trigger of cardiac fibrosis mechanisms in chronic HTP smokers through mTOR activation. The results here collected show how human CSCs exposed to the circulating molecules of exclusive HTP chronic smokers display altered phosphorylation of multiple pathways, increased mTOR pathway activation, and a shift towards a fibrotic phenotype, with reduced release of beneficial paracrine factors and impaired capacity to support angiogenesis. Interestingly, these effects appear different to some extent from those generated by the serum of chronic TCC smokers, inducing intermediate responses for some features

of the phenotype of CSCs. In fact, the serum of TCC smokers caused a much more evident pro-inflammatory profile in CSCs, with significant reduction of migration capacity, and pro-survival signals to cardiomyocytes. Interestingly, the HTP serum affected those properties of CSCs to a lower extent. The distinctive and strong effects in our conditions appeared to be the reduction of Cx43 expression, with increased αSMA expression and collagen release elicited by exposure to the serum of HTP smokers. This raises a worrying alarm against the possible activation of fibrotic pathways in chronic HTP use, known in the literature to contribute to arrhythmogenic effects. Overall, our results suggest that the specific molecular profile in the serum of exclusive HTP smokers may act as an important trigger for the mTOR pathway and subsequent possible activation of fibrotic behavior through the altered functional and paracrine phenotype of resident stromal cells in the atria.

Funding

This work was supported by grant # 20222KETLS from the Italian Ministry of University and Research to IC and FP. This work was partially supported by grant # RG11916B8621D7FF to GBZ, and grant # RM12117A5D7688BC to RC from Sapienza University of Rome. GF is supported by the European Union-NextGenerationEU program through the Italian Ministry of University and Research under PNRR-Project PE06-HEAL ITALIA-SPOKE 1-DSBMC. EDF is supported by grant "Progetto ECS 0000024 Rome Technopole, CUP B83C22002820006, PNRR Missione 4 Componente 2 Investimento 1.5", funded by the European Union—NextGenerationEU program.

Disclosures

GBZ has consulted for Cardionovum, Crannmedical, Innovheart, Meditrial, Opsens Medical, Replycare, and Terumo on topics not related to this project. All other authors have nothing to disclose.

CRediT authorship contribution statement

Vittorio Picchio: Writing – original draft, Methodology, Formal analysis, Data curation, Conceptualization. **Francesca Pagano:** Writing – review & editing, Supervision, Formal analysis, Data curation, Conceptualization. **Roberto Carnevale:** Supervision, Resources, Investigation, Funding acquisition, Conceptualization. **Alessandra D'Amico:** Methodology, Formal analysis, Data curation. **Claudia Cozzolino:** Methodology, Formal analysis, Data curation. **Erica Floris:** Methodology, Data curation. **Antonella Bordin:** Resources, Methodology, Data curation. **Leonardo Schirone:** Resources, Data curation. **Daniele Vecchio:** Methodology, Data curation. **Wael Saade:** Resources, Data curation. **Fabio Miraldi:** Supervision, Resources. **Elena De Falco:** Writing – review & editing, Supervision, Methodology, Funding acquisition. **Sebastiano Sciarretta:** Writing – review & editing, Supervision, Methodology. **Mariangela Peruzzi:** Resources, Data curation. **Giuseppe Biondi-Zoccai:** Supervision, Methodology, Funding acquisition. **Giacomo Frati:** Writing – review & editing, Supervision, Resources, Investigation, Funding acquisition, Conceptualization. **Isotta Chimenti:** Writing – review & editing, Writing – original draft, Supervision, Project administration, Methodology, Investigation, Funding acquisition, Formal analysis, Conceptualization.

Declaration of competing interest

The authors declare the following financial interests/personal relationships which may be considered as potential competing interests: Giuseppe Biondi-Zoccai reports a relationship with Cardionovum, Crannmedical, Innovheart, Meditrial, Opsens Medical, Replycare, and Terumo that includes: consulting or advisory. If there are other authors, they declare that they have no known competing financial interests or personal relationships that could have appeared to influence the work reported in this paper.

Data availability

Data included in this manuscript can be available from the corresponding author upon reasonable request.

Appendix A. Supplementary data

Supplementary data to this article can be found online at https://doi.org/10.1016/j.bbadis.2024.167350.

References

[1] A. Goette, U. Lendeckel, A. Kuchenbecker, A. Bukowska, B. Peters, H.U. Klein, C. Huth, C. Röcken, Cigarette smoking induces atrial fibrosis in humans via nicotine, Heart 93 (2007) 1056, https://doi.org/10.1136/HRT.2005.087171.
[2] A. Kaplan, E. Abidi, R. Ghali, G.W. Booz, F. Kobeissy, F.A. Zouein, Functional, cellular, and molecular remodeling of the heart under influence of oxidative cigarette tobacco smoke, Oxid. Med. Cell. Longev. 2017 (2017), https://doi.org/10.1155/2017/3759186.
[3] V. Picchio, A. Bordin, E. Floris, C. Cozzolino, X. Dhori, M. Peruzzi, G. Frati, E. De Falco, F. Pagano, I. Chimenti, E. De Falco, F. Pagano, I. Chimenti, The Dynamic Facets of the Cardiac Stroma: From Classical Markers to Omics and Translational Perspectives, e-Century Publishing Corporation, 2022. www.ajtr.org (accessed March 24, 2022).
[4] M.V. Plikus, X. Wang, S. Sinha, E. Forte, S.M. Thompson, E.L. Herzog, R.R. Driskell, N. Rosenthal, J. Biernaskie, V. Horsley, Fibroblasts: origins, definitions, and functions in health and disease, Cell 184 (2021) 3852–3872, https://doi.org/10.1016/J.CELL.2021.06.024.
[5] E. Forte, M.B. Furtado, N. Rosenthal, The interstitium in cardiac repair: role of the immune–stromal cell interplay, Nat. Publ. Group (2018), https://doi.org/10.1038/s41569-018-0077-x.
[6] F. Pagano, V. Picchio, F. Angelini, A. Iaccarino, M. Peruzzi, E. Cavarretta, G. Biondi-Zoccai, S. Sciarretta, E. De Falco, I. Chimenti, G. Frati, The biological mechanisms of action of cardiac progenitor cell therapy, Curr. Cardiol. Rep. 20 (2018) 1–10, https://doi.org/10.1007/s11886-018-1031-6.
[7] T. Jerzyński, G.V. Stimson, H. Shapiro, G. Król, Estimation of the global number of e-cigarette users in 2020, Harm Reduct. J. 18 (2021), https://doi.org/10.1186/S12954-021-00556-7.
[8] G. Biondi-Zoccai, R. Carnevale, S. Sciarretta, G. Frati, Electronic cigarette, European Heart Journal Supplements: Journal of the European Society of Cardiology 22 (2020) E25, https://doi.org/10.1093/EURHEARTJ/SUAA053.
[9] G. Biondi-Zoccai, S. Sciarretta, C. Bullen, C. Nocella, F. Violi, L. Loffredo, P. Pignatelli, L. Perri, M. Peruzzi, A.G.M. Marullo, E. De Falco, I. Chimenti, V. Cammisotto, V. Valenti, F. Coluzzi, E. Cavarretta, A. Carrizzo, F. Prati, R. Carnevale, G. Frati, Acute effects of heat-not-burn, electronic vaping, and traditional tobacco combustion cigarettes: the Sapienza University of Rome-vascular assessment of proatherosclerotic effects of smoking (SUR-VAPES) 2 randomized trial, J. Am. Heart Assoc. 8 (2019), https://doi.org/10.1161/JAHA.118.010455.
[10] L. Loffredo, R. Carnevale, S. Battaglia, R. Marti, S. Pizzolo, S. Bartimoccia, C. Nocella, V. Cammisotto, S. Sciarretta, I. Chimenti, E. De Falco, E. Cavarretta, M. Peruzzi, A. Marullo, F. Miraldi, F. Violi, A. Morelli, G. Biondi-Zoccai, G. Frati, Impact of Chronic Use of Heat-Not-Burn Cigarettes on Oxidative Stress, Endothelial Dysfunction and Platelet Activation: The SUR-VAPES Chronic Study, (n.d.). doi: https://doi.org/10.1136/thoraxjnl-2020-215900.
[11] V. Picchio, G. Ferrero, C. Cozzolino, B. Pardini, E. Floris, S. Tarallo, X. Dhori, C. Nocella, L. Loffredo, G. Biondi-Zoccai, R. Carnevale, G. Frati, I. Chimenti, F. Pagano, Effect of traditional or heat-not-burn cigarette smoking on circulating miRNAs in healthy subjects, Eur. J. Clin. Invest. 54 (2024) e14140, https://doi.org/10.1111/ECI.14140.
[12] W.H. Lee, S.G. Ong, Y. Zhou, L. Tian, H.R. Bae, N. Baker, A. Whitlatch, L. Mohammadi, H. Guo, K.C. Nadeau, M.L. Springer, S.F. Schick, A. Bhatnagar, J. C. Wu, Modeling cardiovascular risks of E-cigarettes with human-induced pluripotent stem cell-derived endothelial cells, J. Am. Coll. Cardiol. 73 (2019) 2722–2737, https://doi.org/10.1016/J.JACC.2019.03.476.
[13] A. Merecz-Sadowska, P. Sitarek, H. Zielinska-Blizniewska, K. Malinowska, K. Zajdel, L. Zakonnik, R. Zajdel, A Summary of In Vitro and In Vivo Studies Evaluating the Impact of E-Cigarette Exposure on Living Organisms and the Environment, Int. J. Mol. Sci. Vol. 21 (2020) 652, https://doi.org/10.3390/IJMS21020652.
[14] C. Cozzolino, V. Picchio, E. Floris, F. Pagano, W. Saade, M. Peruzzi, G. Frati, I. Chimenti, Modified risk tobacco products and cardiovascular repair: still very smoky, Curr. Stem Cell Res. Ther. 17 (2022), https://doi.org/10.2174/1574888X17666220802142532.
[15] I. Chimenti, R. Gaetani, E. Forte, F. Angelini, E. De Falco, G.B. Zoccai, E. Messina, G. Frati, A. Giacomello, Serum and supplement optimization for <scp>EU GMP</scp> −compliance in cardiospheres cell culture, J. Cell. Mol. Med. 18 (2014) 624–634, https://doi.org/10.1111/jcmm.12210.
[16] I. Chimenti, F. Pagano, E. Cavarretta, F. Angelini, M. Peruzzi, A. Barretta, E. Greco, E. De Falco, A.G.M. Marullo, S. Sciarretta, G. Biondi-Zoccai, G. Frati, B-blockers

treatment of cardiac surgery patients enhances isolation and improves phenotype of cardiosphere-derived cells, Sci. Rep. 6 (2016) 1–13, https://doi.org/10.1038/srep36774.
[17] F. Pagano, V. Picchio, A. Bordin, E. Cavarretta, C. Nocella, C. Cozzolino, E. Floris, F. Angelini, A. Sordano, M. Peruzzi, F. Miraldi, G. Biondi-Zoccai, E. De Falco, R. Carnevale, S. Sciarretta, G. Frati, I. Chimenti, Progressive stages of dysmetabolism are associated with impaired biological features of human cardiac stromal cells mediated by the oxidative state and autophagy, J. Pathol. (2022), https://doi.org/10.1002/path.5985.
[18] I. Belviso, F. Angelini, F. Di Meglio, V. Picchio, A.M. Sacco, C. Nocella, V. Romano, D. Nurzynska, G. Frati, C. Maiello, E. Messina, S. Montagnani, F. Pagano, C. Castaldo, I. Chimenti, The microenvironment of decellularized extracellular matrix from heart failure myocardium alters the balance between angiogenic and fibrotic signals from stromal primitive cells, Int. J. Mol. Sci. 21 (2020) 1–18, https://doi.org/10.3390/IJMS21217903.
[19] G. Garoffolo, M. Casaburo, F. Amadeo, M. Salvi, G. Bernava, L. Piacentini, I. Chimenti, G. Zaccagnini, G. Milcovich, E. Zuccolo, M. Agrifoglio, S. Ragazzini, O. Baasansuren, C. Cozzolino, M. Chiesa, S. Ferrari, D. Carbonaro, R. Santoro, M. Manzoni, L. Casalis, A. Raucci, F. Molinari, L. Menicanti, F. Pagano, T. Ohashi, F. Martelli, D. Massai, G.I. Colombo, E. Messina, U. Morbiducci, M. Pesce, Reduction of cardiac fibrosis by interference with YAP-dependent transactivation, Circ. Res. 131 (2022) 239–257, https://doi.org/10.1161/CIRCRESAHA.121.319373.
[20] N.E. Ryu, S.H. Lee, H. Park, Spheroid culture system methods and applications for mesenchymal stem cells, Cells 8 (2019), https://doi.org/10.3390/CELLS8121620.
[21] V.M. Mahoney, V. Mezzano, G.R. Mirams, K. Maass, Z. Li, M. Cerrone, C. Vasquez, A. Bapat, M. Delmar, G.E. Morley, Connexin43 contributes to electrotonic conduction across scar tissue in the intact heart, Sci. Rep. 6 (2016), https://doi.org/10.1038/SREP26744.
[22] E. Giacomelli, V. Meraviglia, G. Campostrini, A. Cochrane, X. Cao, R.W.J. van Helden, A. Krotenberg Garcia, M. Mircea, S. Kostidis, R.P. Davis, B.J. van Meer, C. R. Jost, A.J. Koster, H. Mei, D.G. Míguez, A.A. Mulder, M. Ledesma-Terrón, G. Pompilio, L. Sala, D.C.F. Salvatori, R.C. Slieker, E. Sommariva, A.A.F. de Vries, M. Giera, S. Semrau, L.G.J. Tertoolen, V.V. Orlova, M. Bellin, C.L. Mummery, Human-iPSC-Derived Cardiac Stromal Cells Enhance Maturation in 3D Cardiac Microtissues and Reveal Non-cardiomyocyte Contributions to Heart Disease, Cell Stem Cell 26 (2020) 862, https://doi.org/10.1016/J.STEM.2020.05.004.
[23] V. Nagibin, T. Egan Benova, C. Viczenczova, B. Szeiffova Bacova, I. Dovinova, M. Barancik, N. Tribulova, N. Tribulová, Ageing related down-regulation of myocardial Connexin-43 and up-regulation of MMP-2 may predict propensity to atrial fibrillation in experimental animals, Physiol. Res. 65 (2016) 91–100, https://doi.org/10.33549/physiolres.933389.
[24] J. Yan, J.K. Thomson, W. Zhao, X. Wu, X. Gao, D. DeMarco, W. Kong, M. Tong, J. Sun, M. Bakhos, V.G. Fast, Q. Liang, S.D. Prabhu, X. Ai, The stress kinase JNK regulates gap junction Cx43 gene expression and promotes atrial fibrillation in the aged heart, J. Mol. Cell. Cardiol. 114 (2018) 105–115, https://doi.org/10.1016/J.YJMCC.2017.11.006.
[25] J.H. Rennison, L. Li, C.R. Lin, B.S. Lovano, L. Castel, S.Y. Wass, C.C. Cantlay, M. McHale, A.M. Gillinov, R. Mehra, B.B. Willard, J.D. Smith, M.K. Chung, J. Barnard, D.R. Van Wagoner, Atrial fibrillation rhythm is associated with marked changes in metabolic and Myofibrillar protein expression in left atrial appendage, Pflugers Archiv: European Journal of Physiology 473 (2021) 461, https://doi.org/10.1007/S00424-021-02514-5.
[26] J. Cao, D. Xu, D. Wang, R. Wu, L. Zhang, H. Zhu, Q. He, B. Yang, ROS-driven Akt dephosphorylation at Ser-473 is involved in 4-HPR-mediated apoptosis in NB4 cells, Free Radic. Biol. Med. 47 (2009) 536–547, https://doi.org/10.1016/J.FREERADBIOMED.2009.05.024.
[27] S.G. Rhee, Y.S. Bae, S.R. Lee, J. Kwon, Hydrogen peroxide: a key messenger that modulates protein phosphorylation through cysteine oxidation, Sci. STKE 2000 (2000), https://doi.org/10.1126/STKE.2000.53.PE1.
[28] C. Wen, H. Wang, X. Wu, L. He, Q. Zhou, F. Wang, S. Chen, L. Huang, J. Chen, H. Wang, W. Ye, W. Li, X. Yang, H. Liu, J. Peng, ROS-mediated inactivation of the PI3K/AKT pathway is involved in the antigastric cancer effects of thioredoxin reductase-1 inhibitor chaetocin, Cell Death Dis. 10 (2019), https://doi.org/10.1038/S41419-019-2035-X.
[29] Z. Feng, A.J. Levine, The regulation of energy metabolism and the IGF-1/mTOR pathways by the p53 protein, Trends Cell Biol. 20 (2010) 427–434, https://doi.org/10.1016/j.tcb.2010.03.004.
[30] J.C. Garbern, A. Helman, R. Sereda, M. Sarikhani, A. Ahmed, G.O. Escalante, R. Ogurlu, S.L. Kim, J.F. Zimmerman, A. Cho, L. MacQueen, V.J. Bezzerides, K. K. Parker, D.A. Melton, R.T. Lee, Inhibition of mTOR signaling enhances maturation of cardiomyocytes derived from human induced pluripotent stem cells via p53-induced quiescence, Circulation 141 (2020) 285, https://doi.org/10.1161/CIRCULATIONAHA.119.044205.
[31] K.S. Kovacina, G.Y. Park, S.S. Bae, A.W. Guzzetta, E. Schaefer, M.J. Birnbaum, R. A. Roth, Identification of a proline-rich Akt substrate as a 14-3-3 binding partner, J. Biol. Chem. 278 (2003) 10189–10194, https://doi.org/10.1074/jbc.M210837200.
[32] H. Lal, F. Ahmad, J. Woodgett, T. Force, The GSK-3 family as therapeutic target for myocardial diseases, Circ. Res. 116 (2015) 138, https://doi.org/10.1161/CIRCRESAHA.116.303613.
[33] J. Lawrence, R. Nho, Molecular Sciences The Role of the Mammalian Target of Rapamycin (mTOR) in Pulmonary Fibrosis, (n.d.). doi:https://doi.org/10.3390/ijms19030778.
[34] C. Wiza, E.B.M. Nascimento, D. Margriet, Role of PRAS40 in Akt and mTOR signaling in health and disease, Am. J. Physiol. Endocrinol. Metab. 302 (2012) 1453–1460, https://doi.org/10.1152/ajpendo.00660.2011.-The.
[35] S. Sciarretta, M. Volpe, J. Sadoshima, Mammalian target of rapamycin signaling in cardiac physiology and disease, Circ. Res. 114 (2014) 549–564, https://doi.org/10.1161/CIRCRESAHA.114.302022.
[36] R. Jagannathan, S.A. Patel, M.K. Ali, K.M.V. Narayan, MACROVASCULAR COMPLICATIONS IN DIABETES (VR ARODA AND A GETANEH, SECTION EDITORS) Global Updates on Cardiovascular Disease Mortality Trends and Attribution of Traditional Risk Factors, 2019, https://doi.org/10.1007/s11892-019-1161-2.
[37] A.A. Laverty, C.I. Vardavas, F.T. Filippidis, Prevalence and reasons for use of heated tobacco products (HTP) in Europe: an analysis of Eurobarometer data in 28 countries, The Lancet Regional Health - Europe 8 (2021) 100159, https://doi.org/10.1016/j.lanepe.2021.100159.
[38] C. Haig, D. Carrick, J. Carberry, K. Mangion, A. Maznyczka, K. Wetherall, M. McEntegart, M.C. Petrie, H. Eteiba, M. Lindsay, S. Hood, S. Watkins, A. Davie, A. Mahrous, I. Mordi, N. Ahmed, V. Teng Yue May, I. Ford, A. Radjenovic, P. Welsh, N. Sattar, K.G. Oldroyd, C. Berry, Current Smoking and Prognosis After Acute ST-Segment Elevation Myocardial Infarction: New Pathophysiological Insights, JACC: Cardiovascular Imaging vol. 12, 2019, pp. 993–1003, https://doi.org/10.1016/J.JCMG.2018.05.022.
[39] Q. Wang, Y. Song, J. Chen, Q. Li, J. Gao, H. Tan, Y. Zhu, Z. Wang, M. Li, H. Yang, N. Zhang, X. Li, J. Qian, Z. Pang, Z. Huang, J. Ge, Direct in vivo reprogramming with non-viral sequential targeting nanoparticles promotes cardiac regeneration, Biomaterials 276 (2021) 121028, https://doi.org/10.1016/j.biomaterials.2021.121028.
[40] Y. Bei, Q. Zhou, Q. Sun, J. Xiao, Telocytes in cardiac regeneration and repair, Semin. Cell Dev. Biol. 55 (2016) 14–21, https://doi.org/10.1016/j.semcdb.2016.01.037.
[41] L. Wang, T.E. Harris, R.A. Roth, J.C. Lawrence, PRAS40 regulates mTORC1 kinase activity by functioning as a direct inhibitor of substrate binding, J. Biol. Chem. 282 (2007) 20036–20044, https://doi.org/10.1074/jbc.M702376200.
[42] A. Beà, J.G. Valero, A. Irazoki, C. Lana, G. López-Lluch, M. Portero-Otín, P. Pérez-Galán, J. Inserte, M. Ruiz-Meana, A. Zorzano, M. Llovera, D. Sanchis, Cardiac fibroblasts display endurance to ischemia, high ROS control and elevated respiration regulated by the JAK2/STAT pathway, FEBS J. 289 (2022) 2540–2561, https://doi.org/10.1111/FEBS.16283.
[43] S. Comità, S. Femmino, C. Thairi, G. Alloatti, K. Boengler, P. Pagliaro, C. Penna, Regulation of STAT3 and its role in cardioprotection by conditioning: focus on non-genomic roles targeting mitochondrial function, Basic Research in Cardiology 116 (2021) 1–31, https://doi.org/10.1007/S00395-021-00898-0.
[44] M.O. Lee, K.B. Jung, S.J. Jo, S.A. Hyun, K.S. Moon, J.W. Seo, S.H. Kim, M.Y. Son, Modelling cardiac fibrosis using three-dimensional cardiac microtissues derived from human embryonic stem cells, J. Biol. Eng. 13 (2019), https://doi.org/10.1186/S13036-019-0139-6.